Charge Transfer Kinetics in Fullerene−Oligomer−Fullerene Triads Containing Alkylpyrrole Units

Edwin H. A. Beckers,[†] Paul A. van Hal,[†] Anantharaman Dhanabalan,[†] Stefan C. J. Meskers,[†] Joop Knol,[‡] J. C. Hummelen,[‡] and René A. J. Janssen*[,†]

Laboratory of Macromolecular and Organic Chemistry, Eindhoven University of Technology, P.O. Box 513, 5600 MB Eindhoven, The Netherlands, and Stratingh Institute and MSC, University of Groningen, Nijenborgh 4, 9747 AG Groningen, The Netherlands

Received: May 21, 2003; In Final Form: June 18, 2003

A photoinduced electron-transfer reaction has been observed in three fullerene−donor−fullerene triads containing an electron-rich pyrrole ring in the donor moiety. The kinetics of charge separation in solution has been investigated by photoluminescence and transient absorption spectroscopy. The polarity of solvent and the distance between donor and acceptor affect the forward electron-transfer reaction, in qualitative agreement with a semiempirical model for the Gibbs free energy for charge separation. Depending on the conditions, charge separation occurs at a rate of 10^9-10^{10} s^{-1}. The charge recombination rate is estimated to be faster than 2×10^{10} s^{-1}. The relatively large contribution of the singlet-excited-state $S_n \leftarrow S_1$ absorption of the fullerene moiety to the photoinduced absorption hampered a more accurate determination of the recombination rate.

Introduction

To disclose the complex processes involved in the photoinduced electron-transfer reaction between a π-conjugated donor and a fullerene acceptor, extensive studies have addressed the photophysical properties of covalently linked oligomer−C_{60} diads and triads containing, among others, oligothiophenes,[1] oligo(*p*-phenylenevinylene)s,[2] and porphyrins[3] as the electron donor. Here we report on the charge-transfer kinetics of fullerene−donor−fullerene triads containing a pyrrole unit in the donor. The electron-rich pyrrole unit is used to lower the oxidation potential (E_{ox}) and thereby increase the change in free energy for electron transfer, enabling this reaction to occur in apolar media.

The three novel (ADA) triads used in this study are shown in Figure 1. ADA-1 consists of a thiophene−pyrrole−thiophene (T−Py−T) donor moiety coupled to two *N*-methylfulleropyrrolidine (MP−C_{60}) electron acceptors.[4] ADA-2 has a similar structure as ADA-1, but the two thiophene rings have been replaced by phenyl groups. As a result, the Ph−Py−Ph donor moiety of ADA-2 has approximately the same geometry as ADA-1, but a significantly higher oxidation potential. This allows investigation of the effect of the oxidation potential on photophysical processes without adjusting the distance between the donor and acceptor chromophores. In ADA-3, the T−Py−T donor of ADA-1 is augmented with two phenyl groups on each side, to increase the distance between the donor and acceptor, but without significantly affecting the oxidation potential.

The kinetics for photoinduced charge separation and recombination in the triads have been studied with fluorescence quenching and lifetime spectroscopy in combination with near-steady-state and transient photoinduced absorption (PIA) experiments and have been compared to the electron-transfer reactions observed in mixtures of the donor model compound D1, D2, or D3 with MP−C_{60} (Figure 1).

Experimental Section

Materials. The syntheses of ADA-1, ADA-2, and ADA-3 have been described previously.[5] Each of the three triads consists of a mixture of stereoisomers as a consequence of the stereocenter at each pyrrolidine ring. Compounds D1,[6] D2,[5] and MP−C_{60}[7] have been prepared according to literature procedures.

Preparation of *N*-Dodecyl-2,5-bis(5′-phenyl-2′-thienyl)-pyrrole (D3). Dichlorobis(triphenylphosphine)palladium(II) (7 mg, 1 mol %) was added to a stirred mixture of *N*-dodecyl-2,5-bis(5′-trimethylstannyl-2′-thienyl)pyrrole[5] (0.40 g, 1 mmol) and bromobenzene (0.36 g, 2.3 mmol) in dry THF (15 mL). The mixture was stirred at 85 °C under argon for 15 h. Subsequently, the dark-red reaction mixture was poured into a mixture of water and diethyl ether. The organic layer was washed three times with water, dried over $MgSO_4$, and concentrated in vacuo to yield a dark-red semisolid mass in 80% yield. The crude product was further purified by column chromatography (SiO_2, *n*-hexane/dichloromethane 60:40) to yield a yellow powder. ^{1}H NMR ($CDCl_3$, 400 MHz): δ (ppm) 7.65, 7.42, 7.32 (m, 10H, PhH), 7.31 (d, 2H, TH, $J = 4.0$ Hz), 7.06 (d, 2H, TH, $J = 4.0$ Hz), 6.43 (s, 2H, PyH), 4.26 (t, 2H, NCH_2), 1.67 (m, 2H, NCH_2CH_2), 1.26 (m, 18H, $(CH_2)_9$), 0.90 (t, 3H, CH_3). ^{13}C NMR ($CDCl_3$, 100 MHz): δ (ppm) 143.9, 134.6, 134.5, 134.4, 129.2, 129.0, 125.9, 123.5, 126.8, 111.2, 45.6, 32.2, 31.4, 29.9, 29.9, 29.8, 29.7, 29.6, 29.2, 26.7, 22.9, 14.4.

Electrochemistry. Cyclic voltammograms were measured in dichloromethane ($\epsilon = 8.93$), with 0.1 M tetrabutylammonium hexafluorophosphate ($TBAPF_6$) as a supporting electrolyte, using a Potentioscan Wenking POS73 potentiostat. The working electrode was a Pt disk (0.2 cm^2), the counter electrode was a

* Corresponding author. Phone: (+)31.40.2473597. Fax: (+)31.40.2451036. E-mail: r.a.j.janssen@tue.nl.
† Eindhoven University of Technology.
‡ University of Groningen.

10.1021/jp035402i CCC: $25.00
Published on Web 07/22/2003

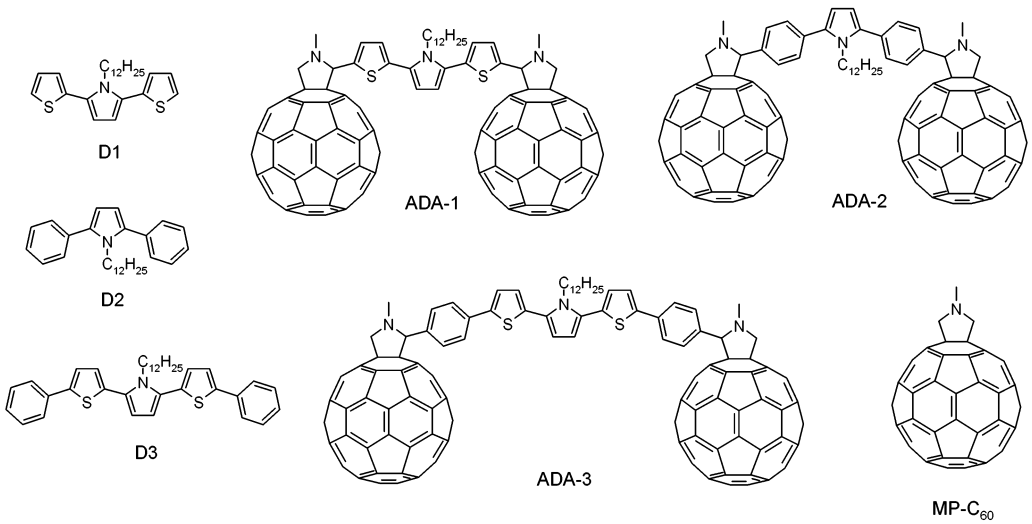

Figure 1. Studied compounds: donor molecules D1, D2, and D3; triads ADA-1, ADA-2, and ADA-3; MP−C_{60}.

Pt plate (0.5 cm^2), and a saturated calomel electrode (SCE) was used as the reference electrode, calibrated against Fc/Fc^+ (0.46 V).

Absorption and Fluorescence Spectroscopy. UV/vis absorption and fluorescence spectra were recorded with a Perkin-Elmer Lambda 40 spectrometer and an Edinburgh Instruments FS920 double-monochromator luminescence spectrometer using a Peltier-cooled red-sensitive photomultiplier, respectively. All UV/vis and fluorescence measurements were carried out in 10 mm quartz cells. Solvents for absorption and fluorescence measurements were used as received. Oxidation experiments were carried out under inert conditions by adding a solution of thianthrenium perchlorate[8] in dichloromethane via a syringe through a Teflon-lined septum sealing the substrate solution.

Time-Correlated Single Photon Counting. Time-correlated single photon counting fluorescence studies were performed using an Edinburgh Instruments LifeSpec-PS spectrometer. The LifeSpec-PS comprises a 400 nm picosecond laser (PicoQuant PDL 800B) operated at 2.5 MHz and a Peltier-cooled Hamamatsu microchannel plate photomultiplier (R3809U-50). Lifetimes were determined from the data using the Edinburgh Instruments software package.

Near-Steady-State PIA. Solutions containing 2×10^{-4} M of each compound were prepared in a nitrogen-filled glovebox to exclude interference of oxygen during measurements. The PIA spectra were recorded between 0.5 and 3.0 eV by exciting with a mechanically modulated cw Ar ion laser ($\lambda = 528$ nm, 275 Hz) pump beam and monitoring the resulting change in transmission of a tungsten−halogen probe light through the sample (ΔT) with a phase-sensitive lock-in amplifier after dispersion by a grating monochromator and detection, using Si, InGaAs, and cooled InSb detectors. The pump power incident on the sample was typically 25 mW with a beam diameter of 2 mm. The PIA ($-\Delta T/T \approx \Delta\alpha d$) was directly calculated from the change in transmission after correction for the photoluminescence, which was recorded in a separate experiment. Photoinduced absorption spectra and photoluminescence spectra were recorded with the pump beam in a direction almost parallel to the direction of the probe beam. The solutions were studied in a 1 mm near-IR grade quartz cell at room temperature. Solvents for PIA measurements were distilled under nitrogen before use.

Transient Subpicosecond Photoinduced Absorption. The femtosecond laser system used for pump−probe experiments consisted of an amplified Ti/sapphire laser (Spectra Physics Hurricane). The single pulses from a cw mode-locked Ti/sapphire laser were amplified by a Nd:YLF laser using chirped pulse amplification, providing 150 fs pulses at 800 nm with an energy of 750 μJ and a repetition rate of 1 kHz. The pump pulses at 455 nm were created via optical parametric amplification (OPA) of the 800 nm pulse by a BBO crystal into infrared pulses which were then two times frequency doubled via BBO crystals. The probe beam was generated in a separate optical parametric amplification setup in which the 900 and 1030 nm pulses were created and a RG 850 nm cutoff filter was used to avoid contributions of residual probe light (800 nm) from the OPA. The pump beam was focused to a spot size of about 1 mm^2 with an excitation flux of 1 $mJ \cdot cm^{-2}$ per pulse. The probe beam was reduced in intensity compared to the pump beam by using neutral density filters. The pump beam was linearly polarized at the magic angle of 54.7° with respect to the probe, to cancel out orientation effects in the measured dynamics. The temporal evolution of the differential transmission was recorded using a Si detector by a standard lock-in technique at 500 Hz.

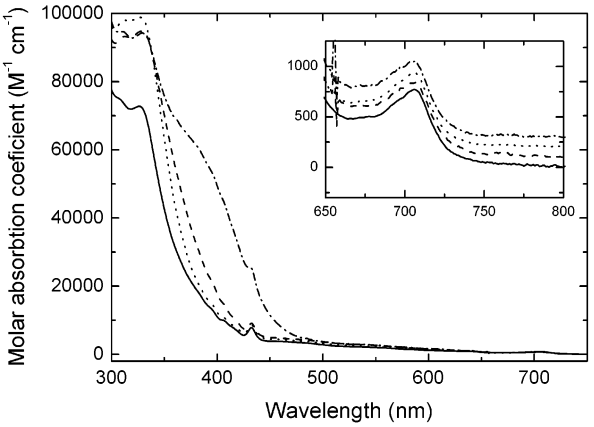

Figure 2. UV/vis absorption spectra of MP−C_{60} (solid line) and the triads ADA-1 (dashed line), ADA-2 (dotted line), and ADA-3 (dash−dotted line) in ODCB. The inset shows the spectra in the 650−800 nm region. In the inset the spectra are offset vertically for clarity.

Results and Discussion

Energy Levels. The UV/vis spectra (Figure 2) of the three triads exhibit characteristic absorption peaks at 433 and 705

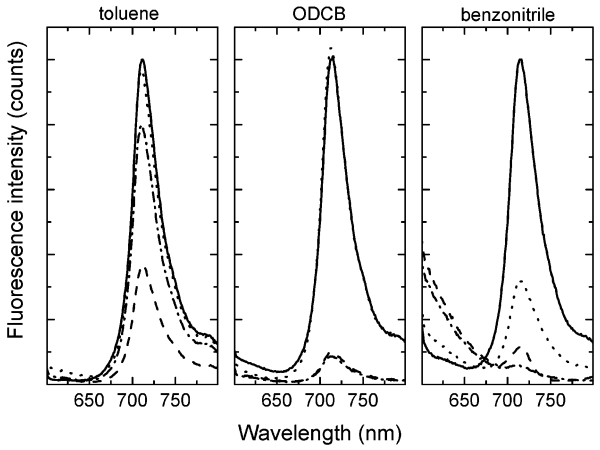

Figure 3. Fluorescence spectra of MP−C_{60} (solid line) and the triads ADA-1 (dashed line), ADA-2 (dotted line), and ADA-3 (dash−dotted line) in toluene (left), ODCB (middle), and benzonitrile (right). Excitation was at 500 nm, all spectra are corrected for optical density.

nm of the fulleropyrrolidine moiety. Compared to MP−C_{60}, ADA-1 and ADA-3 exhibit additional absorptions in the UV region, as a result of the contribution of the conjugated donor segments. The spectra were found to be independent of the polarity of the solvent. The UV/vis spectra of the triads only show absorptions that are also present in the isolated chromophores and they represent the sum of the spectra of the donors (D1, D2, and D3) and MP−C_{60}. This indicates that the electronic coupling between the donor and acceptor chromophores in the ground state is weak. However, because the spectra of the donor (D1, D2, and D3) and MP−C_{60} partially overlap, small changes that have occurred in the region where the spectra coincide cannot be excluded. The spectra demonstrate that the lowest singlet excited state in the ADA triads is localized on the fulleropyrrolidine unit at 1.76 eV (∼705 nm).

The donor molecules undergo a reversible electrochemical oxidation at potentials 0.83, 1.02, and 0.73 V (versus SCE in CH_2Cl_2) for D1, D2, and D3, respectively. Compared to similarly substituted thiophene molecules (1.07 V for 3T (terthiophene), 1.42 V for Ph−T−Ph, and 0.96 for Ph−3T−Ph), [1f,9] the introduction of the pyrrole unit reduces the oxidation potential considerably.

Photoluminescence Quenching. The intensity of the fullerene photoluminescence (PL) of the triads at 712 nm can be used to assess whether an intramolecular charge-transfer reaction occurs from the donor to the fullerene acceptor. Figure 3 compares the PL of the fulleropyrrolidine group in the triads to that of MP−C_{60} in three solvents of increasing polarity. The observed PL quenching for ADA-1 indicates that charge transfer already occurs in a relatively apolar solvent such as toluene ($\epsilon = 2.38$). The ADA-2 molecule exhibits no PL quenching in toluene, because the high oxidation potential inhibits a photoinduced electron transfer. The PL quenching of ADA-3 in toluene is less than for ADA-1, despite its slightly lower oxidation potential. We attribute this difference to the increased distance between the pyrrole and the fullerene groups in ADA-3 as compared to ADA-1, which increases the energy of the charge-separated state. With increasing polarity of the solvent (ODCB: $\epsilon = 9.93$; benzonitrile $\epsilon = 25.2$), the fullerene emission of the triads is increasingly quenched (Figure 3, Table 2).

The rate constant for charge separation (k_{CS}) can be determined from the PL lifetime of MP−C_{60} and the fulleropyrrolidine PL quantum yield of the triad molecules (ϕ) compared to that of MP−C_{60} ($\phi(C_{60})$), via

$$k_{CS} = \left[\frac{\phi(C_{60})}{\phi} - 1\right]/\tau(MP - C_{60}) \qquad (1)$$

The resulting values indicate that k_{CS} is in the range 10^9-10^{10} s^{-1}, depending on the nature of the triad and the solvent (Table 2).

TABLE 1: Change in Gibbs Free Energy for Charge Separation (ΔG_{CS}) in Toluene (TOL), *o*-Dichlorobenzene (ODCB), and Benzonitrile (BZN), Calculated Using Eq 2 for *Intra*molecular Electron Transfer in ADA Triads Relative to the MP−C_{60}(S_1) State (E_{00} = 1.76 eV) and for *Inter*molecular ($R_{cc} = \infty$) Electron Transfer in D/MP−C_{60} Mixtures Relative to the MP−C_{60}(T_1) State (E_{00} = 1.50 EV)[a]

sample	solvent	R_{cc} (Å)	ΔG_{CS} (eV)
ADA-1	TOL	10.5	0.11
	ODCB	10.5	−0.43
	BZN	10.5	−0.54
ADA-2	TOL	11.0	0.57
	ODCB	11.0	−0.25
	BZN	11.0	−0.40
ADA-3	TOL	14.0	0.15
	ODCB	14.0	−0.50
	BZN	14.0	−0.62
D1 + MP−C_{60}	TOL	∞	0.95
	ODCB	∞	−0.03
	BZN	∞	−0.22
D3 + MP−C_{60}	TOL	∞	0.85
	ODCB	∞	−0.13
	BZN	∞	−0.32

[a] The center-to-center distance (R_{cc}) has been listed; other parameters are described in the text.

TABLE 2: Fullerene Fluorescence Quenching Factors, $\phi(C_{60})/\phi$, Fullerene PL Lifetime, τ_{obs}, and Rate Constants for Charge Separation, k_{CS}, Calculated with Eqs 1 and 3

compound	solvent	$\phi(C_{60})/\phi$	k_{CS} (s^{-1})[a]	τ_{obs} (ns)	k_{CS} (s^{-1})[b]
ADA-1	TOL	2.7	1.2×10^9	0.77	0.6×10^9
	ODCB	10.1	7.0×10^9	0.12	7.6×10^9
	BZN	8.8	5.3×10^9	n.d.	
ADA-2	TOL	1.0	$\ll 10^8$	1.43	$< 10^7$
	ODCB	1.0	$\ll 10^8$	1.19	0.08×10^9
	BZN	3.2	1.5×10^9	n.d.	
ADA-3	TOL	1.3	1.7×10^8	1.53	*c*
	ODCB	11.5	8.0×10^9	0.12	7.6×10^9
	BZN	17.8	1.2×10^{10}	n.d.	
MP−C_{60}	TOL			1.45	
	ODCB			1.31	
	BZN			1.46	

[a] Calculated from $\phi(C_{60})/\phi$ and eq 1. [b] Calculated from τ_{obs} and eq 3. [c] Electron transfer is slow, using eq 3 would yield a negative value.

Gibbs Free Energy for Charge Separation. The experimental results can be rationalized using a semiquantitative model[10] (eq 2) that provides an estimate for the change in Gibbs free energy for charge separation. In this equation, E_{ox} and E_{red} represent the oxidation and reduction potential of respectively the donor and the acceptor, measured in a solvent with relative permittivity ϵ_{ref}. E_{00} is the energy of the excited state from which the electron transfer occurs, whereas e and ϵ_0 are the electron charge and the vacuum permittivity. R_{cc} is the center-to-center distance between the positive and the negative charges in the charge-separated state and r^+ and r^- indicate the radii of the cation and anion. The radius of the negative ion of C_{60} was set to $r^- = 5.6$ Å.[1f] The radii of the radical cations of D1 and D3 are assumed to be equal to the r^+ value for unsubstituted

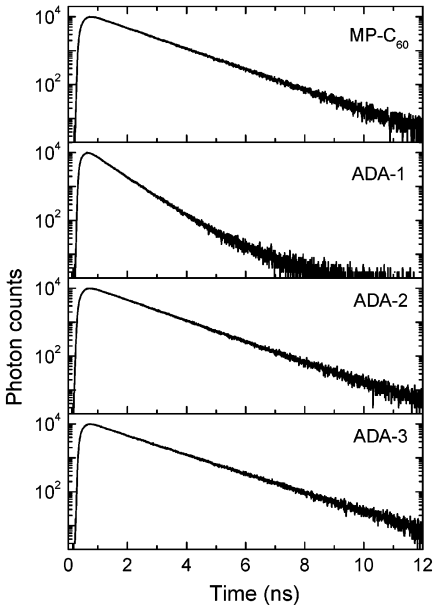

Figure 4. Fluorescence lifetime of MP−C_{60} and ADA triads measured at 711 nm in toluene. Excitation was at 400 nm.

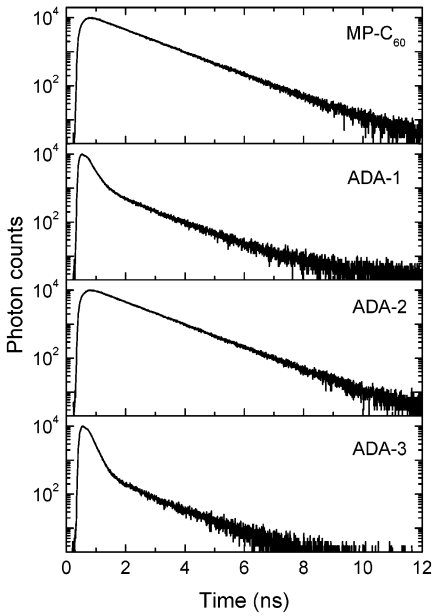

Figure 5. Fluorescence lifetime of MP−C_{60} and ADA triads measured at 714 nm in ODCB. Excitation was at 400 nm.

terthiophene (4.03 Å),[1f] because the contribution of the phenyl group to the charge distribution is assumed to be negligible.[6] The radius for D2 is calculated to be 2.8 Å, assuming that the charge is mainly localized on the pyrrole ring.

$$\Delta G_{CS} = e[E_{ox}(D) - E_{red}(A)] - E_{00} - \frac{e^2}{4\pi\epsilon_0\epsilon_s R_{cc}} - \frac{e^2}{8\pi\epsilon_0}\left(\frac{1}{r^+} + \frac{1}{r-}\right)\left(\frac{1}{\epsilon_{ref}} - \frac{1}{\epsilon_s}\right) \quad (2)$$

Using $R_{cc} = 10.5$ Å, the charge-separated state for ADA-1 in toluene appears to be slightly higher in energy than the MP−C_{60}(S_1) state (Table 1). This result disagrees with the experimental observations, but charge transfer becomes exergonic when R_{cc} is (slightly) reduced to 9 Å. In agreement with the experimental results, the energy of the charge-separated states for ADA-2 and ADA-3 in toluene are higher than that of ADA-1 and the MP−C_{60}(S_1) state. In more polar solvents, photoinduced electron transfer becomes increasingly exergonic for all triads, in agreement with the observed PL quenching (Figure 3). One other disagreement between the predictions from eq 2 and the experiment must be noted. The PL intensity of ADA-2 in ODCB is equal to that of MP−C_{60}, indicating an absence of charge separation, whereas the charge-separated state is predicted to be −0.25 eV below the MP−C_{60}(S_1) state.[11]

Time-Resolved Photoluminescence. Time-resolved PL measurements have been used to obtain the rate of a charge separation, independent from the PL intensity quenching, by detecting a change in the decay rate of the fulleropyrrolidine singlet state in the triads compared to MP−C_{60}. In toluene solutions, a decrease of the fullerene PL lifetime is indeed observed for ADA-1, whereas the PL time profiles of ADA-2 and ADA-3 are identical to that of MP−C_{60} (Figure 4). In ODCB, the decay of both ADA-1 and ADA-3 is faster than that of MP−C_{60} (Figure 5). PL lifetimes have been determined with a biexponential curve fitting procedure in which one time constant was kept constant at the singlet lifetime of MP−C_{60} in the same solvent.[12] The rate constants for charge separation, calculated from the fluorescence lifetimes using eq 3 are similar to those obtained from the steady-state luminescence experiments (Table 2).

$$k_{CS} = \frac{1}{\tau_{obs}} - \frac{1}{\tau(MP - C_{60})} \quad (3)$$

In addition to the rate constants, also the energy barrier ($\Delta G^{\ddagger}$) for photoinduced electron transfer has been determined for ADA-1 and ADA-3 in ODCB by temperature-dependent fluorescence lifetime experiments. By using the semiclassical Marcus equation,[13] the temperature dependence of the electron-transfer rate can be described with

$$\ln(k_{CS}T^{1/2}) = \ln\left(\frac{2\pi^{3/2}|V|^2}{h(\lambda k_B)^{1/2}}\right) - \frac{\Delta G^{\ddagger}}{k_B T} \quad (4)$$

The energy barriers in ODCB, calculated from the slope ($-\Delta G^{\ddagger}/k_B$) of a modified Arrhenius plot[14] (Figure 6), amount to 0.088 and 0.084 eV for ADA-1 and ADA-3, respectively.[15] The experimental energy barriers can be compared to the barriers that can be obtained using eq 5. In eq 5, λ represents the

$$\Delta G^{\ddagger} = \frac{(\Delta G_{CS} + \lambda)^2}{4\lambda} \quad (5)$$

reorganization energy, which is the sum of the internal (λ_i) and solvent (λ_s) reorganization.[13] The internal reorganization is set to 0.3 eV,[4] whereas the solvent contribution can be calculated using the Born-Hush[16] approach (eq 6). For ODCB as solvent,

$$\lambda_s = \frac{e^2}{4\pi\epsilon_0}\left(\frac{1}{2}\left(\frac{1}{r^+} + \frac{1}{r-}\right) - \frac{1}{R_{cc}}\right)\left(\frac{1}{n^2} - \frac{1}{\epsilon_s}\right) \quad (6)$$

this approximation results in $\lambda_s = 0.53$ eV and $\Delta G^{\ddagger} = 0.048$ eV for ADA-1 and $\lambda_s = 0.64$ eV and $\Delta G^{\ddagger} = 0.052$ eV for ADA-3. These energy barriers are similar to the experimentally determined values. The reorganization energies of 0.83 and 0.94 eV imply that $-\Delta G_{CS}$ is less than λ, such that the forward electron-transfer reaction occurs in the Marcus normal region.[13] Using λ and the intercept of the modified Arrhenius plot, the electronic coupling matrix elements are determined to be 26 cm^{-1} for both ADA-1 and ADA-3 in ODCB. This result is

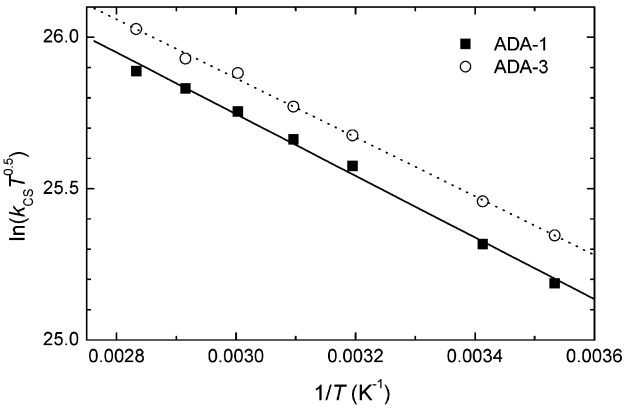

Figure 6. Modified Arrhenius plot of $\ln(k_{CS}T^{0.5})$ versus $1/T$ (K^{-1}) for ADA-1 and ADA-3 in ODCB. The lines represent the linear fit of the experimental data to obtain the energy barrier $\Delta G^{\ddagger}$ for the charge-transfer reaction.

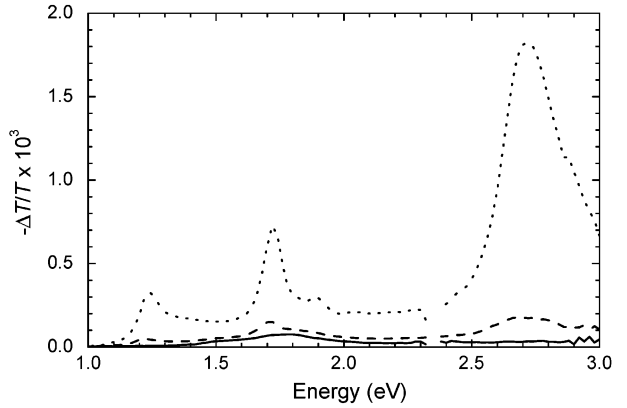

Figure 7. Photoinduced absorption spectra of 2×10^{-4} M mixtures of D1 and MP−C_{60} in toluene (solid line), ODCB (dashed line), and benzonitrile (dotted line). Excitation was at 528 nm (2.35 eV).

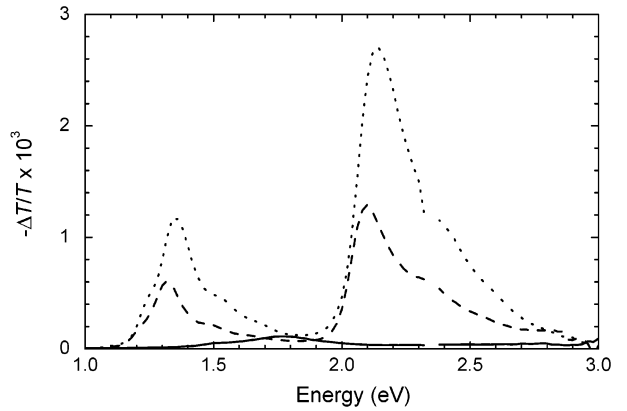

Figure 8. Photoinduced absorption spectra of 2×10^{-4} M mixtures of D3 and MP−C_{60} in toluene (solid line), ODCB (dashed line), and benzonitrile (dotted line). Excitation was at 528 nm (2.35 eV).

identical to the value previously reported for oligomer−fullerene compounds.[4,17]

Near-Steady-State Photoinduced Absorption. To determine the absorption spectra of the radical cations of D1 and D3, near-steady-state PIA experiments were performed on 2×10^{-4} M solution of these donor molecules together with an equimolar amount of MP−C_{60} (Figure 7, Figure 8).[18] In these experiments selective excitation of the fullerene chromphore at 528 nm results in the formation of the MP−C_{60} triplet state, which may react intermolecularly with D1 or D3 to give a radical ion pair. The PIA spectra of D1/MP−C_{60} and D3/MP−C_{60} in toluene

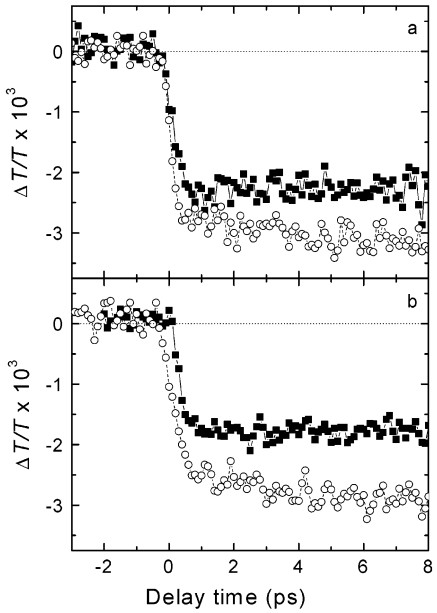

Figure 9. Differential transmission dynamics at (a) 1030 nm and (b) 900 nm of ADA-1 (solid squares) and ADA-3 (open circles) in ODCB from −3 to +8 ps. Recorded with excitation at 455 nm.

both show the typical MP−C_{60} triplet−triplet absorption with a maximum at 1.78 eV.[19] Apparently, *inter*molecular charge separation does not occur in toluene, consistent with the Gibbs free energies for charge transfer calculated with eq 2 (Table 1). In ODCB and benzonitrile, the increased polarity lowers the Gibbs free energy of the charge-separated state below the energy of the MP−$C_{60}(T_1)$ state from which the intermolecular electron transfer occurs. The PIA spectrum of D1/MP−C_{60} shows three absorptions bands at 1.24, 1.72, and 2.72 eV, respectively. The band at 1.24 eV is highly characteristic of the MP−$C_{60}^{\bullet-}$ radical anion;[20] the other two are assigned to absorptions of the $D1^{\bullet+}$ radical cation. The PIA spectrum of the D3/MP−C_{60} mixture shows peaks at 1.33 and 2.13 eV, which are assigned to $D3^{\bullet+}$ absorptions. The low-energy absorption shows a shoulder at 1.24 eV, again indicating the presence of MP−$C_{60}^{\bullet-}$.

Transient Photoinduced Absorption. In addition to the (time-resolved) PL experiments, which provide rate constants for the forward charge separation reaction, transient PIA can be used to study the dynamics of charge formation and recombination when the absorption of the radical cations or anions are monitored in time. The transient differential absorption at 1030 nm (1.2 eV) of ADA-3 in ODCB was recorded to investigate the dynamics of the formation and decay of $C_{60}^{\bullet-}$ radical anions. The signal reaches its maximum within 1 ps (Figure 9), i.e., comparable to the width of the used laser pulse, and then decays exponentially with a time constant of 127 ps (Figure 10). The subpicosecond rise indicates that at 1030 nm the differential transmission is probably not only due to $C_{60}^{\bullet-}$ radical anions, because these are formed at a much lower rate (Table 2). Remarkably, the time constant of the decay of the differential transmission at 1030 nm is identical to the lifetime of the $C_{60}(S_1)$ state in ADA-3, as determined by PL lifetime measurements (Table 2). Because both fluorescence and electron transfer occur from the $C_{60}(S_1)$ state, the PL lifetime of ADA-3 corresponds to the generation of $C_{60}^{\bullet-}$ radical anions and not to their decay. We therefore propose that the 1030 nm differential transmission signal does not primarily relate to the $C_{60}^{\bullet-}$ radical anion but rather originates predominantly from the C_{60} $S_n \leftarrow S_1$ absorption. To investigate this in more detail, the differential transmission at 900 nm has also been recorded.

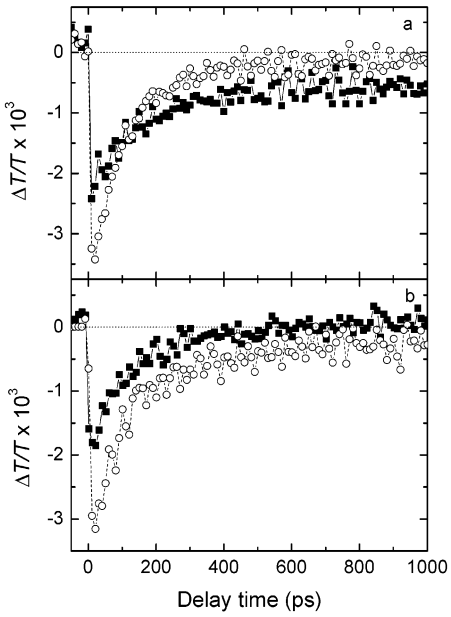

Figure 10. Differential transmission dynamics at (a) 1030 nm and (b) 900 nm of ADA-1 (solid squares) and ADA-3 (open circles) in ODCB from −50 to +1000 ps. Recorded with excitation at 455 nm.

The molar absorption coefficient of the MP−C_{60} $S_n \leftarrow S_1$ transition (9000 L·mol^{-1}·cm^{-1}) is twice as high as the absorption coefficient of the MP−C_{60} radical anion (5000 L·mol^{-1}·cm^{-1}) at this wavelength.[19] The results at 900 nm are similar to those at 1030 nm, exhibiting a rise in less than 1 ps and a decay with a time constant of 107 ps (Figure 9, Figure 10).

The near-steady-state absorption spectra of D1 or D3 with MP−C_{60} in ODCB (Figure 7) show that the absorption at 1030 nm is 4 times larger for the D3/MP−C_{60} mixture as compared to the D1/MP−C_{60} mixture. However, the transient differential transmission profiles at 900 and 1030 nm of ADA-1 in ODCB show only minor differences compared to the profiles of ADA-3 in ODCB. After a rise of the signal within 1 ps, the signals show an exponential decay with time constants of 156 and 135 ps at 900 and 1030 nm, respectively (Figures 9 and 10). Although these values are slightly higher than the observed fluorescence lifetime of 118 ps, they support the view that the transient PIA signal is predominantly a result of the excited-state $S_n \leftarrow S_1$ absorption of MP−C_{60}.

Using the absorption coefficients of the charge-separated state and the excited-state $S_n \leftarrow S_1$ absorption of MP−C_{60} at 900 nm in ODCB, the time profile of the transient differential absorption after excitation can be calculated as a function of the rate constants for intrinsic decay (k_0), charge separation (k_{CS}), and charge recombination (k_{CR}) (Figure 11).[21] In this model, charge separation is assumed to occur exclusively from the MP−$C_{60}(S_1)$ state and the rate for charge recombination is varied, while k_0 and k_{CS} are kept constant at the experimental values.[21] From the steady-state PIA experiments it can be concluded that there is no significant absorption of the radical cation for the ADA-1 triad at 900 nm; therefore the absorption coefficient of the charged species is equal to that of MP−$C_{60}^{\bullet-}$ (5000 L·mol^{-1}·cm^{-1}).[19] The molar absorption coefficient of the radical cation of ADA-3 has been determined from the absorption spectrum of D3$^{\bullet+}$, which was obtained by oxidizing D3 with thianthrenium perchlorate.[8] At 900 nm, the molar absorption coefficient for D3$^{\bullet+}$ is 14000 L·mol^{-1}·cm^{-1}. The ratio of the absorption coefficients at 900 nm (1.38 eV) of the MP−$C_{60}(S_1)$ state and the charge-separated state (CSS) were therefore set at 9000:5000 for ADA-1 and at 9000:19000 for ADA-3.[22]

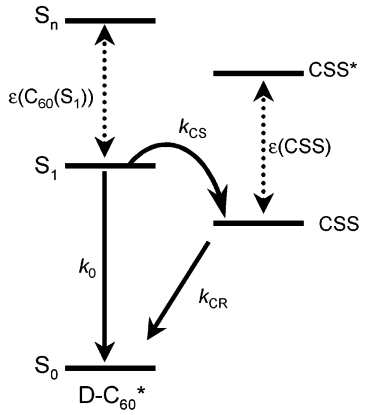

Figure 11. Energy diagram for the charge-transfer reaction (k_{CS}) from the MP−$C_{60}(S_1)$ state to the charge-separated state (CSS) together with intrinsic (k_0) and charge recombination (k_{CR}) decay pathways.

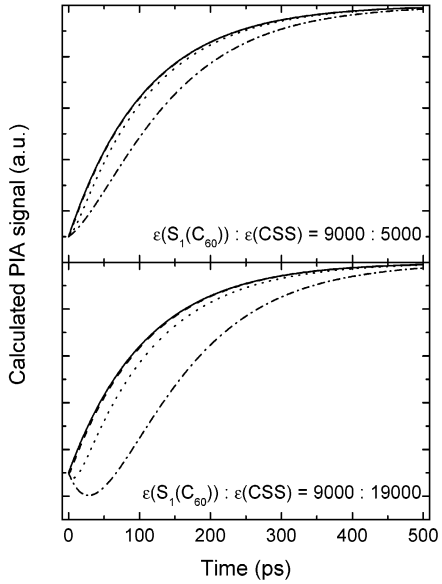

Figure 12. Calculated differential transmission at 900 nm for charge recombination rate constants of 1 ps^{-1} (dashed line), 0.1 ps^{-1} (dotted line), and 0.02 ps^{-1} (dash−dotted line), compared to the decay of the MP−$C_{60}(S_1)$ state (solid line). The spectra are calculated with the model illustrated in Figure 11 with $\epsilon(C_{60}(S_1)):\epsilon(CSS) = 9000:5000$ (top) and $\epsilon(C_{60}(S_1)):\epsilon(CSS) = 9000:19000$ (bottom). The used values for k_{CS} and k_0 correspond to time constants of 120 and 1310 ps, respectively.

The calculated time profiles for values of k_{CR} ranging from 10^{12} to 2×10^{10} s^{-1} (Figure 12) clearly reveal that as long as charge recombination is faster than 2×10^{10} s^{-1} (50 ps), the transient signal is dominated by the $S_n \leftarrow S_1$ absorption of the MP−$C_{60}(S_1)$ state, even if the absorption coefficient of the charge-separated state is higher than the singlet-excited-state absorption. Under these conditions the transient signal is indistinguishable from the $S_n \leftarrow S_1$ absorption of MP−C_{60}, which hampers an accurate analysis of the recombination dynamics.[23] This is a general problem in donor−fullerene systems: the overlap of the $S_n \leftarrow S_1$ and radical anion absorptions of the fullerene in the 800−1100 nm region complicates the investigation of formation and recombination kinetics.

Because the experimentally obtained time profiles are similar to the modeled curves with fast recombination, we estimate that charge recombination in ADA-1 and ADA-3 occurs within 50

ps ($k_{CR} > 2 \times 10^{10}$ s^{-1}). This is in agreement with rate constants obtained for comparable thiophene−MP−C_{60} diads and triads.[1g,2e]

Conclusion

Intramolecular photoinduced electron transfer has been observed in three fullerene−donor−fullerene (ADA) triads that contain an electron-rich pyrrole ring in the donor moiety. The charge-transfer kinetics have been studied in solution with PL and transient PIA spectroscopy. In agreement with a semiquantitative model for the Gibbs free energy for charge separation, the photoinduced charge transfer depends on the polarity of the solvent and the distance between donor and fullerene acceptor. Although charge separation occurs for ADA-1 in toluene, a higher polarity solvent is required to generate a photoinduced charge-separated state in ADA-2 and ADA-3. PL quenching and time-resolved PL studies reveal that the rate for charge separation in the ADA triads is in the range $k_{CS} = 10^9 - 10^{10}$ s^{-1}. Near-steady-state PIA in mixtures of the donor model compounds D1 or D3 with MP−C_{60} reveal that an intermolecular charge transfer occurs from the MP−C_{60}(T_1) state, evidenced by the observation of the absorption spectra of the corresponding radical ions in the near-infrared. Transient PIA in the picosecond time domain for the triads, recorded at the near-infrared absorption wavelengths of the radical ions, produced a signal that was dominated by the excited-state $S_n \leftarrow S_1$ absorption of the MP−C_{60} moiety. A kinetic model, involving the relative absorption coefficients of the excited states, explains this behavior when the charge recombination is faster than the charge separation. A semiquantitative analysis suggests that the recombination rate, k_{CR}, is larger than 2×10^{10} s^{-1} (lifetime < 50 ps).

Acknowledgment. This work is supported by the Council for Chemical Sciences of The Netherlands Organization for Scientific Research (CW-NWO) in the PIONIER program (98400). The research of S.C.J.M. has also been made possible by a fellowship of the Royal Dutch Academy of Arts and Sciences.

References and Notes

(1) (a) Benincori, T.; Brenna, E.; Sannicolo, F.; Trimarco, L.; Zotti, G.; Sozzani, P. *Angew. Chem., Int. Ed. Engl.* **1996**, *35*, 648. (b) Effenberger; F.; Grube, G. *Synthesis* **1998**, 1372. (c) Knorr, S.; Grupp, A.; Mehring, M.; Grube, G.; Effenberger, F. *J. Chem. Phys.* **1999**, *110*, 3502. (d) Yamashiro, T.; Aso, Y.; Otsubo, T.; Tang, H.; Harima, Y.; Yamashita, K. *Chem. Lett.* **1999**, 443. (e) Fujitsuka, M.; Ito, O.; Yamashiro, T.; Aso, Y.; Otsubo, Y. *J. Phys. Chem. A* **2000**, *104*, 4876. (f) van Hal, P. A.; Knol, J.; Langeveld-Voss, B. M. W.; Meskers, S. C. J.; Hummelen, J. C.; Janssen, R. A. J. *J. Phys. Chem. A* **2000**, *104*, 5974. (g) van Hal, P. A.; Janssen, R. A. J.; Lanzani, G.; Cerullo, G.; Zavelani-Rossi, M.; De Silvestri, S. *Chem. Phys. Lett.* **2001**, *345*, 33. (h) Fujitsuka, M.; Masahura, A.; Kasai, H.; Oikawa, H.; Nakanishi, H.; Ito, O.; Yamashiro, T.; Aso, Y.; Otsubo, T. *J. Phys. Chem. B* **2001**, *105*, 9930. (i) Fujitsuka, M.; Matsumoto, K.; Ito, O.; Yamashiro, T.; Aso, Y.; Otsubo, T. *Res. Chem. Intermed.* **2001**, *27*, 73. (j) Hirayama, D.; Takimiya, K.; Aso, Y.; Otsubo, T. Hasobe, T.; Yamada, H. Imahori, H.; Fukuzumi, S.; Sakata, Y. *J. Am. Chem. Soc.* **2002**, *124*, 532. (k) van Hal, P. A.; Beckers, E. H. A.; Meskers, S. C. J.; Janssen, R. A. J.; Jousselme, B.; Blanchard, P.; Roncali, J. *Chem. Eur. J.* **2002**, *8*, 5415.

(2) (a) Nierengarten, J. F.; Eckert, J. F.; Nicoud, J. F.; Ouali, L.; Krasnikov, V.; Hadziioannou, G. *Chem. Commun.* **1999**, 617. (b) Eckert, J. F.; Nicoud, J. F.; Nierengarten, J. F.; Liu, S. G.; Echegoyen, L.; Barigelletti, F.; Armaroli, N.; Ouali, L.; Krasnikov, V. V.; Hadziioannou, G. *J. Am. Chem. Soc.* **2000**, *122*, 7467. (c) Armaroli, N.; Barigelletti, F.; Ceroni, P.; Eckert, J.-F.; Nicoud, J.-F.; Nierengarten, J.-F. *Chem. Commun.* **2000**, 599. (d) Peeters, E.; van Hal, P. A.; Knol, J.; Brabec, C. J.; Sariciftci, N. S.; Hummelen, J. C.; Janssen, R. A. J. *J. Phys. Chem. B* **2000**, *104*, 10174. (e) van Hal, P. A.; Janssen, R. A. J.; Lanzani, G.; Cerullo, G.; Zavelani-Rossi, M.; De Silvestri, S. *Phys. Rev. B* **2001**, *64*, 075206. (f) Nierengarten, J.-F.; Armaroli, N.; Accorsi, G.; Rio, Y.; Eckert, J.-F. *Chem. Eur. J.* **2003**, *9*, 37.

(3) For recent reviews see: (a) Gust, D.; Moore, T. A.; Moore, A. L. *Acc. Chem. Res.* **2001**, *34*, 40. (b) Guldi, D. M. *Chem. Soc. Rev.* **2002**, *31*, 22.

(4) Williams, R. M.; Zwier, J. M.; Verhoeven, J. W. *J. Am. Chem. Soc.* **1995**, *117*, 4093.

(5) Dhanabalan, A.; Knol, J.; Hummelen, J. C.; Janssen, R. A. J. *Synth. Met.* **2001**, *119*, 519.

(6) van Haare, J. A. E. H.; Groenendaal, L.; Peerlings, H. W. I.; Havinga, E. E.; Vekemans, J. A. J. M.; Janssen, R. A. J.; Meijer, E. W. *Chem. Mater.* **1995,** *7*, 1984.

(7) Maggini, M.; Scorrano, G.; Prato, M. *J. Am. Chem. Soc.* **1993**, *115*, 9798.

(8) Murata, Y.; Shine, H. J. *J. Org. Chem.* **1969**, *34*, 3368.

(9) Apperloo, J. J.; Groenendaal, L.; Verheyen, H.; Jayakannan, M.; Janssen, R. A. J.; Dkhissi, A.; Beljonne, D.; Lazzaroni, R.; Brédas, J. L. *Chem. Eur. J.* **2002**, *8*, 2384.

(10) Weller, A. *Z. Phys. Chem. (Wiesbaden)* **1982**, *133*, 93.

(11) The apparent failure of eq 2 in correctly predicting the energy of the charge-separated state for ADA-2, is tentatively attributed to two inaccuracies: (i) The relatively short distance between donor and acceptor moieties results in an unrealistic estimate of Coulomb term when using eq 2, because the electrostatic attraction of positive and negative charges depends on the actual charge distribution, which is not accurately represented by point charges at the centers of donor and acceptor as assumed in eq 2. (ii) The last term of eq 2 assumes that donor and acceptor are fully solvated. For a small-sized donor positioned between two large fullerene moieties, complete solvation is unlikely.

(12) This contribution is a result of a small fluorescent impurity and typically accounts for less than 5% of the total signal.

(13) (a) Marcus, R. A. *J. Chem. Phys.* **1965**, *43*, 679. (b) Marcus, R. A. *Angew. Chem.* **1993**, *105*, 1161.

(14) (a) Zeng, Y.; Zimmt, M. B. *J. Phys. Chem.* **1992**, *96*, 8395. (b) Komamine, S.; Fujitsuka, M.; Ito, O.; Moriwaki, K.; Miyata, T.; Ohno, T. *J. Phys. Chem. A* **2000**, *104*, 11497. (c) Yamazaki, M.; Araki, Y.; Fujitsuka, M.; Ito, O. *J. Phys. Chem. A* **2001**, *105*, 8615.

(15) Calculated under the assumption that both the reorganization energy and the barrier are temperature independent. In addition, the temperature dependence of the solvent polarity is assumed to have an insignificant effect on the Gibbs free energy for the electron-transfer reaction.

(16) (a) Oevering, H.; Paddon-Row: M. N.; Heppener, M.; Oliver, A. M.; Cotsaris, E.; Verhoeven, J. W.; Hush, N. S. *J. Am. Chem. Soc.* **1987**, *109*, 3258. (b) Kroon, J.; Verhoeven, J. W.; Paddon-Row: M. N.; Oliver, A. M. *Angew. Chem., Int. Ed. Engl.* **1991**, *30*, 1358.

(17) Williams, R. M.; Koeberg, M.; Lawson, J. M.; An, Y. Z.; Rubin, Y.; Paddon-Row: M. N.; Verhoeven, J. W. *J. Org. Chem.* **1996**, *61*, 5055.

(18) With this technique it is not possible to detect charges formed in the triads because near-steady-state PIA operates in the microsecond to millisecond time domain and is orders of magnitude slower than the intramolecular charge recombination.

(19) Guldi, D. M.; Prato, M. *Acc. Chem. Res.* **2000**, *33*, 695.

(20) Guldi, D. M.; Hungerbühler, H.; Janata, E.; Asmus, K. D. *J. Phys. Chem.* **1993**, *97*, 11258.

(21) The intensity of the differential transmission at 900 nm equals the sum of the signals of the C_{60} singlet excited state and the charge-separated state (CSS) via: $\Delta T \propto -\{\epsilon(C_{60}(S_1))[C_{60}(S_1)] + \epsilon(CSS)[CSS]\}$. The concentrations of $C_{60}(S_1)$ and CSS depend on the kinetic constants shown in Figure 11, the initial concentration of $C_{60}(S_1)$ ($[C_{60}(S_1)]_0$) and amount to $[C_{60}(S_1)] = [C_{60}(S_1)]_0 \exp[-(k_{CS} + k_0)t]$ and $[CSS] = [C_{60}(S_1)]_0 \{[k_{CS}/(k_{CR} - k_{CS} - k_0)](\exp[-(k_{CS} + k_0)t] - \exp[-k_{CR}t])\}$, respectively.

(22) For ADA-3, both the cation and anion absorb at 900 nm. Both contributions to the signal are accounted for in the absorption coefficient and the concentration of charged species ([CSS]) is not doubled.

(23) Fujitsuka et al.[1e] previously reported that in picosecond PIA measurements of a quaterthiophene−fulleropyrolidine diad (4T−C_{60}) in an apolar solvent the fulleropyrrolidine $S_n \leftarrow S_1$ excited-state absorption can be observed at wavelengths around 800−1000 nm. However, it was not mentioned that this absorption also contributes to the PIA signal during the formation of the $4T^+ - C_{60}^-$ charge-separated state in more polar solvents.